Radiotherapy Combined with the Immunocytokine L19-IL2 Provides Long-lasting Antitumor Effects

Published OnlineFirst December 31, 2014; DOI: 10.1158/1078-0432.CCR-14-2676

Clinical Cancer Research

Radiotherapy Combined with the Immunocytokine L19-IL2 Provides Long-lasting Antitumor Effects

Catharina M.L. Zegers[1], Nicolle H. Rekers[1], Dana H.F. Quaden[1,2], Natasja G. Lieuwes[1], Ala Yaromina[1], Wilfred T.V. Germeraad[2], Lotte Wieten[3], Erik A.L. Biessen[4], Louis Boon[5], Dario Neri[6], Esther G.C. Troost[1], Ludwig J. Dubois[1], and Philippe Lambin[1]

Abstract

Purpose: Radiotherapy modifies the tumor microenvironment and causes the release of tumor antigens, which can enhance the effect of immunotherapy. L19 targets the extra domain B (ED-B) of fibronectin, a marker for tumor neoangiogenesis, and can be used as immunocytokine when coupled to IL2. We hypothesize that radiotherapy in combination with L19-IL2 provides an enhanced antitumor effect, which is dependent on ED-B expression.

Experimental Design: Mice were injected with syngeneic C51 colon carcinoma, Lewis lung carcinoma (LLC), or 4T1 mammary carcinoma cells. Tumor growth delay, underlying immunologic parameters, and treatment toxicity were evaluated after single-dose local tumor irradiation and systemic administration of L19-IL2 or equimolar controls.

Results: ED-B expression was high, intermediate, and low for C51, LLC, and 4T1, respectively. The combination therapy showed (i) a long-lasting synergistic effect for the C51 model with 75% of tumors being cured, (ii) an additive effect for the LLC model, and (iii) no effect for the 4T1 model. The combination treatment resulted in a significantly increased cytotoxic ($CD8^+$) T-cell population for both C51 and LLC. Depletion of $CD8^+$ T cells abolished the benefit of the combination therapy.

Conclusions: These data provide the first evidence for an increased therapeutic potential by combining radiotherapy with L19-IL2 in ED-B–positive tumors. This new opportunity in cancer treatment will be investigated in a phase I clinical study for patients with an oligometastatic solid tumor (NCT02086721). An animation summarizing our results is available at https://www.youtube.com/watch?v=xHbwQuCTkRc. *Clin Cancer Res; 21(5); 1151–60. ©2014 AACR.*

Introduction

Radiotherapy causes cell-cycle arrest or programmed cell death in rapidly proliferating cancer cells through the induction of DNA damage. In addition, irradiated tumors stimulate the immune system by releasing tumor antigens, damage-associated molecular patterns (DAMP), and through upregulation of immunomodulatory cell surface and secretory molecules (1–4). This promotes the uptake of dying cells by antigen-presenting cells, and provides crosspresentation of the tumor-derived antigens to T cells, thereby triggering a cytotoxic T-lymphocyte response, which might cause immunogenic cell death (ICD; refs. 1, 5, 6). In some cases, tumor growth inhibition outside the field of radiation is observed, termed abscopal effect, which suggests the presence of a systemic radiation-induced antitumor immune response (7–10). However, in general, it is unlikely that radiotherapy alone provides a sufficient antitumor immune response. Therefore, the addition of active immunotherapy may increase the therapeutic potential (11–13).

Active immunotherapy is used to stimulate the immune system acting against tumor cells. Cytotoxic T-lymphocytes and natural killer (NK) cells play an important complementary role in the antitumor immune response as they release specialized lytic granules, which upon interaction with the tumor cell create pores in the lipid bilayer of the target cell resulting in cell death (14, 15). IL2 is a cytokine with an essential role in the activation phase of the immune response; it stimulates the proliferation of cytotoxic T cells, NK cells, and regulatory T cells, providing a balance between a pro- and anti-inflammatory immune response (16–18). Systemic administration of IL2 was introduced as immunotherapy for patients with metastatic melanoma and renal cell carcinoma, which resulted in a higher tumor response and survival (19). However, to reach an effective intratumoral dose of IL2 by systemic administration, high doses ought to be administered, which often leads to toxicity (e.g., capillary leakage syndrome, severe flu-like symptoms, and coma; ref. 20). Currently, intratumoral injections of IL2 are employed to reach a higher local concentration of IL2 (21, 22), which shows promising results in combination with radiotherapy in a preclinical setting (23). However, these intratumoral injections are limited to accessible lesions.

[1]Department of Radiation Oncology (MAASTRO), Maastricht University Medical Centre, Maastricht, the Netherlands. [2]Department of Internal Medicine, Maastricht University Medical Centre, Maastricht, the Netherlands. [3]Department of Transplantation Immunology, Maastricht University Medical Centre, Maastricht, the Netherlands. [4]Experimental Vascular Pathology Group, Cardiovascular Research Institute Maastricht, GROW – School for Oncology and Developmental Biology, Maastricht University Medical Centre, Maastricht, the Netherlands. [5]Bioceros, Utrecht, the Netherlands. [6]Department of Chemistry and Applied Biosciences, Swiss Federal Institute of Technology (ETH Zürich), Zürich, Switzerland.

Note: Supplementary data for this article are available at Clinical Cancer Research Online (http://clincancerres.aacrjournals.org/).

C.M.L. Zegers, N.H. Rekers, L.J. Dubois, and P. Lambin contributed equally to this article.

Corresponding Author: Catharina M.L. Zegers, Maastricht University Medical Centre, Doctor Tanslaan 12, Maastricht 6229ET, the Netherlands. Phone: 318-8445-5666; Fax: 318-8445-5667; E-mail: karen.zegers@maastro.nl

doi: 10.1158/1078-0432.CCR-14-2676

Published OnlineFirst December 31, 2014; DOI: 10.1158/1078-0432.CCR-14-2676

Translational Relevance

Cancer cells have a poor immunogenicity; they are not recognized by the immune system and therefore have the opportunity to survive and proliferate. Radiotherapy causes immunogenic tumor cell death, thereby releasing tumor-associated antigens that can be detected by the immune system, causing an antitumor immune response. Active immunotherapy can be used to further enhance the radiotherapy-induced antitumor immune response. The combination of local radiotherapy to the primary tumor and systemic immunotherapy may therefore activate and stimulate a systemic antitumor response that provides the potential to treat patients with metastatic disease with a curative intent.

An interesting alternative is the selective delivery of IL2 to the tumor by use of fusion proteins (16, 24). During tumor progression, synthesis of extracellular matrix components occurs, with in particular a modulation of vascular cell behavior and angiogenesis (16). Fibronectin of the tumor neovasculature expresses extradomain-B (ED-B), which is preserved in mice, humans, and other mammals. ED-B expression can be used for targeted therapies because it is overexpressed in various solid tumors [e.g., melanoma, renal cell carcinoma (RCC), breast, colorectal, and non–small cell lung cancer], but absent in plasma and normal tissue fibronectin (except for regenerating tissues; refs. 25–30). The small-immuno-protein (SIP) L19 was developed to specifically target the ED-B domain of fibronectin. In previous studies, L19 was used for imaging and targeted (radio)immunotherapy, proving that L19 actually targets the tumor (31–33). Moreover, in phase I clinical studies in patients with metastatic melanoma or RCC, administration of the immunocytokine L19-IL2 alone, or combined with chemotherapy (dacarbazine), was safe and showed clinical activity according to RECIST criteria or progression-free survival (34, 35). Dacarbazine, however, does not have the potential to induce an antitumor immune response, stimulate the exposure of DAMPs, or activate ICD (36), which are all favorable characteristics induced by radiotherapy. Therefore, based on the known immunogenic effects of radiotherapy and the targeted immunostimulating potential of L19-IL2, we hypothesize that the combination of radiotherapy with L19-IL2 will cause an enhanced antitumor effect, which is dependent on the expression of ED-B.

Materials and Methods

Tumor cell lines

Exponentially growing C51 colon carcinoma (kindly provided by Philogen S.p.A.), Lewis lung carcinoma (LLC; kindly provided by G. Molema, UMCG, the Netherlands), and 4T1 mammary carcinoma (ATCC CRL-2539) cell lines were cultured in DMEM (Lonza) supplemented with 10% FCS in a humidified 5% CO_2 chamber at 37°C. All cell lines were directly or indirectly purchased from a cell bank that performs cell line characterizations (short tandem repeat profiling) and were used within 6 months after resuscitation. In addition, cells were tested for mouse antibody production (MAP) and mycoplasma contamination.

Chemicals/reagents/antibodies

The L19-IL2 immunocytokine and L19 (Philogen S.p.A.) were diluted with sterile PBS (Lonza) to concentrations of 200 μg/mL and 133 μg/mL, respectively. IL2 (Proleukin, Novartis) was dissolved as described by the manufacturers' guidelines and diluted with PBS to a concentration of 67 μg/mL.

For the depletion experiments, the anti-CD8 antibody (clone JTS169) and the isotype control (anti-Phyt IgG AFRC MAC 51), kindly provided by Bioceros Bv, were diluted with PBS to a concentration of 2 mg/mL.

Flow cytometric analysis was performed on cells exposed to RBC lysis buffer (eBioscience), FC-block CD16/CD32 (BD Biosciences), and a combination of the antibodies CD3-FITC, CD4-APC-H7, CD8-PE-CY7, CD19-PE, CD45-V500, CD45-Percp, CD45-PE, CD45-FITC, CD45-APC, CD45-PE-CY7, CD3e-eFLUO450, CD4-FITC, CD8a-V500 (BD Biosciences), and NKp46-APC (Miltenyi Biotec B.V.).

In vivo experiments

All experiments were performed in accordance with local institutional guidelines for animal welfare and were approved by the Animal Ethical Committee of the University of Maastricht (Maastricht, the Netherlands). To induce tumors, approximately 8-week-old immunocompetent mice were subcutaneously injected with syngeneic C51 (Balb/c; 1.5×10^6), LLC (C57bl/6; 0.5×10^6), or 4T1 (Balb/c; 1×10^6) tumor cells, resuspended in basement membrane matrix (Matrigel, BD Biosciences). Upon an average tumor volume of 200 mm^3, tumors were irradiated with a single dose (10 Gy for all models, additional groups with 2 and 5 Gy for C51) on day 0, followed by systemic therapy (vehicle PBS/L19 13.3 μg/IL2 6.7 μg/L19-IL2 20 μg) on day 1, 3, and 5. Tumor growth and treatment toxicity (based on body weight) were monitored until reaching 4 times the volume at irradiation time (T4 × SV). Flow cytometry was performed on tumors, spleen, and lymph nodes excised at day 4 of the treatment schedule. Detailed treatment schedules are shown in Supplementary Fig. S1.

To evaluate the causal relationship between the presence of cytotoxic T cells and tumor growth delay, an experimental set up was designed to deplete cytotoxic-T cells in the Balb/c mice bearing C51 tumors. Similar to previous experiments, local irradiation was performed on day 0 (10 Gy) and systemic therapy (vehicle or L19-IL2) was administrated (day 1, 2, 5). In addition, $CD8^+$ cells were depleted by intraperitoneal injection of 0.2 mg (100 μL) anti-CD8 antibody or the negative control anti-Phyt IgG. The timing for the anti-CD8 injections was determined by blood withdrawal, via puncture of the saphenous vein (i) before, (ii) after tumor cell injection, and (iii) 2, 3, or 5 days after injection with the blocking antibodies. The percentage $CD8^+$ cells in the blood was determined as described below. At the end of the experiment, the tumors were harvested for immunohistochemical analysis for CD8 positivity.

Flow cytometry

The number of immune cell subpopulations present in tumor, spleen, and lymph nodes during treatment was analyzed using FACSCanto II flow cytometry (FACS, BD Biosciences). Single-cell suspensions of the tissues were obtained using the gentleMACS dissociator and the tumor dissociation

Published OnlineFirst December 31, 2014; DOI: 10.1158/1078-0432.CCR-14-2676

kit (Miltenyi Biotec B.V.) according to manufacturer's guidelines. Of the acquired single-cell suspension, 1.0×10^6 cells were suspended in FACS buffer (PBS + 1% FCS) for analysis. Cells were incubated with FC-block to avoid nonspecific binding, and staining was performed using the antibodies CD3-FITC, CD4-APC-H7, CD8-PE-CY7, CD19-PE, NKp46-APC, and CD45-V500. The total $CD45^+$ immune cells were selected from the viable population of cells (filtered for debris and doublets) for further subclassification according to the strategy described in Supplementary Fig. S2.

To determine the efficacy of anti-CD8 blocking antibody on the presence of specific immune subpopulations, collected blood was incubated with RBC lysis buffer and FC-block. Next, cells were incubated with CD45-Percp, CD3e-eFLUO450, CD4-FITC, CD8a-V500, NKp46-APC, and CD19-PE, and FACS and data analysis was performed (Supplementary Fig. S3).

Immunofluorescence

To investigate baseline ED-B expression, 7-mm cryostat sections of C51, LLC, and 4T1 tumors were fixed in acetone (4°C) and stained according to previous published methods (37). In brief, sections were incubated with the purified antibodies L19-SIP or KSF-SIP (2 μg/mL; Philochem), with rabbit anti-human-IgE (Dako) and subsequently detected using goat anti-rabbit IgG Alexa Fluor 488 (Life Technologies). Blood vessels and cell nuclei were detected with rat anti-mouse CD31 (BD Biosciences) followed by donkey anti-rat Alexa 594 (Life Technologies) and DAPI (Life Technologies), respectively.

To quantify the ED-B expression, 3 to 12 photomicrographs (805.5 μ × 805.5 μ), depending on tumor size, from viable tumor regions in the largest tumor cross-section were acquired using an Olympus BX51WI fluorescence microscope equipped with a Hamamatsu EM-CCD C9100 digital camera, a motorized stage (Ludl Mac 2000), and a 10× objective. Micromanager 1.4 software was used for automated image acquisition (38). All image recordings were performed with the same settings and analyzed by an investigator blinded to the subject coding. Images were processed using ImageJ software v.1.49b (NIH, Bethesda, MD). The mean fluorescent intensity after correction for cutting and staining artefacts per image was averaged over all images per section to obtain ED-B intensity per tumor.

For the detection of $CD8^+$ T cells residing in tumors, sections were first incubated with anti-CD8 (clone 53.62.7, Department of Pathology, MUMC, Maastricht, the Netherlands) and visualized with goat anti-rabbit IgG Alexa Fluor 488 (Life Technologies). DAPI was used as nuclear counterstain.

Statistical analysis

Statistical analyses were performed using GraphPad Prism Software (v5.03). For all parameters, mean ± SD are reported. The nonparametric Mann–Whitney test was used to determine the statistical differences between the different treatment groups. The log-rank (Mantel–Cox) test was used to compare the survival curves. We used a two-way ANOVA to test the interaction (synergism) between radiotherapy and L19-IL2. A P value smaller than 0.05 was considered statistically significant.

Results

Representative sections of the ED-B expression in the C51, LLC, and 4T1 tumors and their respective fluorescent intensity, corrected for the intensity of the negative controls are shown in Fig. 1. We observed a high, intermediate, and low ED-B expression for the C51 (451 ± 99), LLC (326 ± 70), and 4T1 models (157 ± 143), which were significantly different from each other (all $P < 0.01$). On the basis of body weight measurements and animal welfare monitoring, no toxicity was observed in any of the treatment combinations.

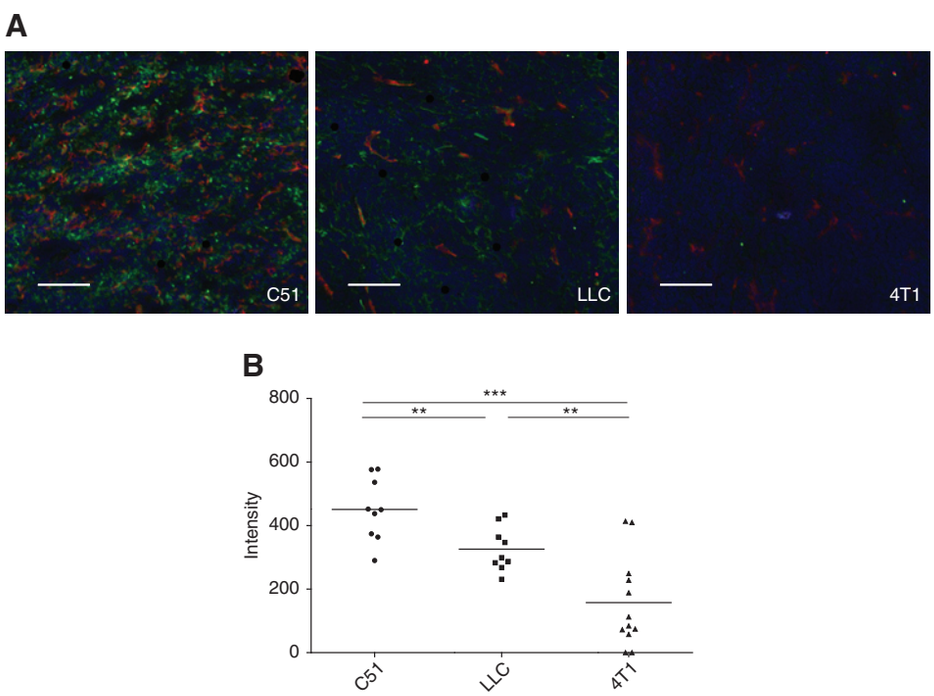

Figure 1.
High, intermediate, and low ED-B expressing tumor models. A, ED-B expression for C51 colon carcinoma, Lewis lung carcinoma (LLC), and 4T1 mammary carcinoma. ED-B expression is detected by L19(sip) biotinylated (green), vessels by anti-CD31 (red), and cell nuclei (DAPI staining) in blue. Scale bar, 100 μm. B, quantification of the ED-B expression (intensity) is corrected for negative control [KSF(sip) biotinylated]. **, $P < 0.01$; ***, $P < 0.001$.

Published OnlineFirst December 31, 2014; DOI: 10.1158/1078-0432.CCR-14-2676

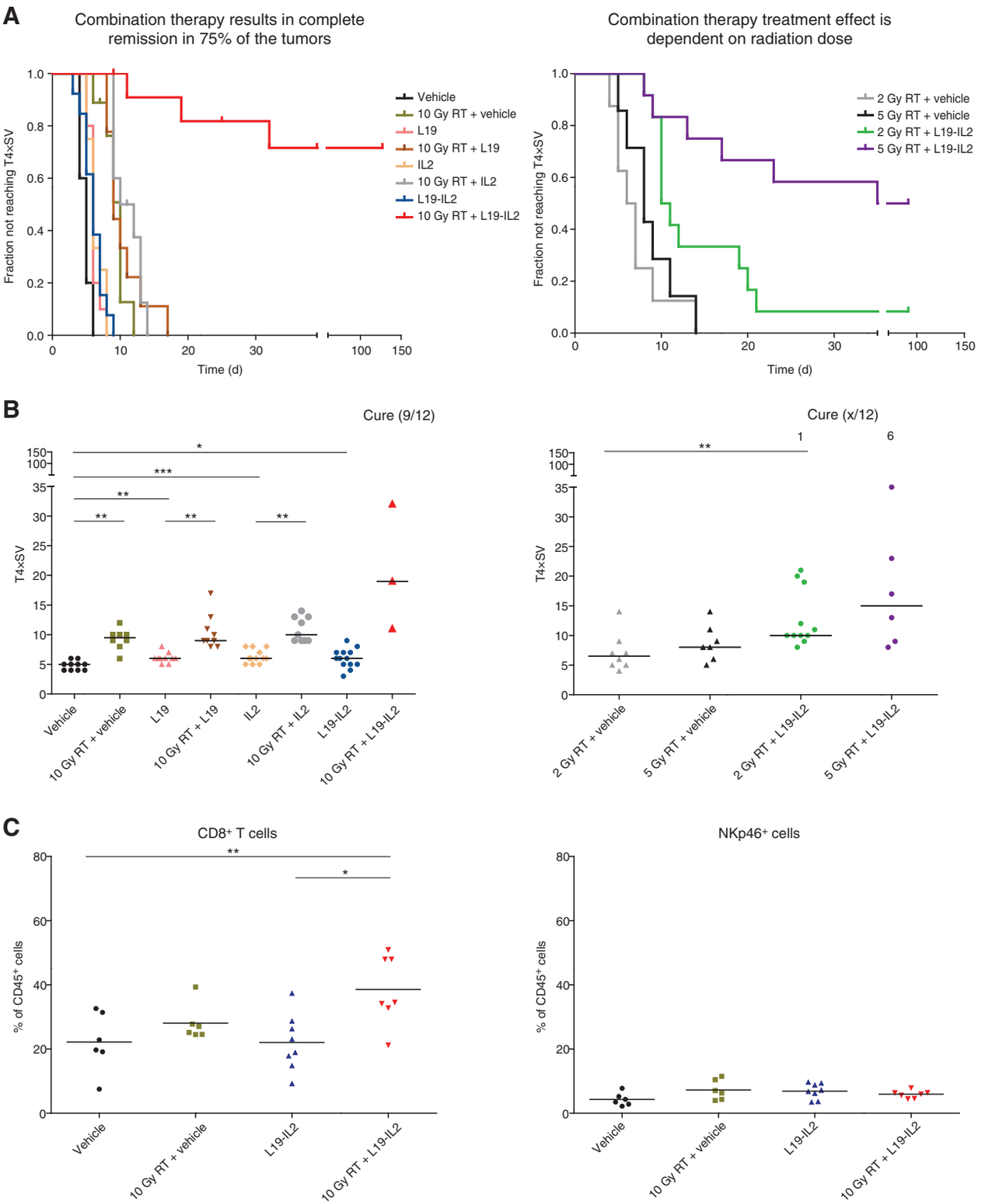

Figure 2.
Combination therapy results in complete remission of 75% in the C51 model. A, fraction of tumors not reaching 4 times start volume (T4 × SV). B, time to reach 4 times start volume for the different treatment groups. C, results of flow cytometry analysis; shown is the percentage of $CD8^+$ and $NKp46^+$ cells of all $CD45^+$ cells present in the tumor. Data represent the mean of 6 to 12 tumors. *, $P < 0.05$; **, $P < 0.01$; ***, $P < 0.001$.

Published OnlineFirst December 31, 2014; DOI: 10.1158/1078-0432.CCR-14-2676

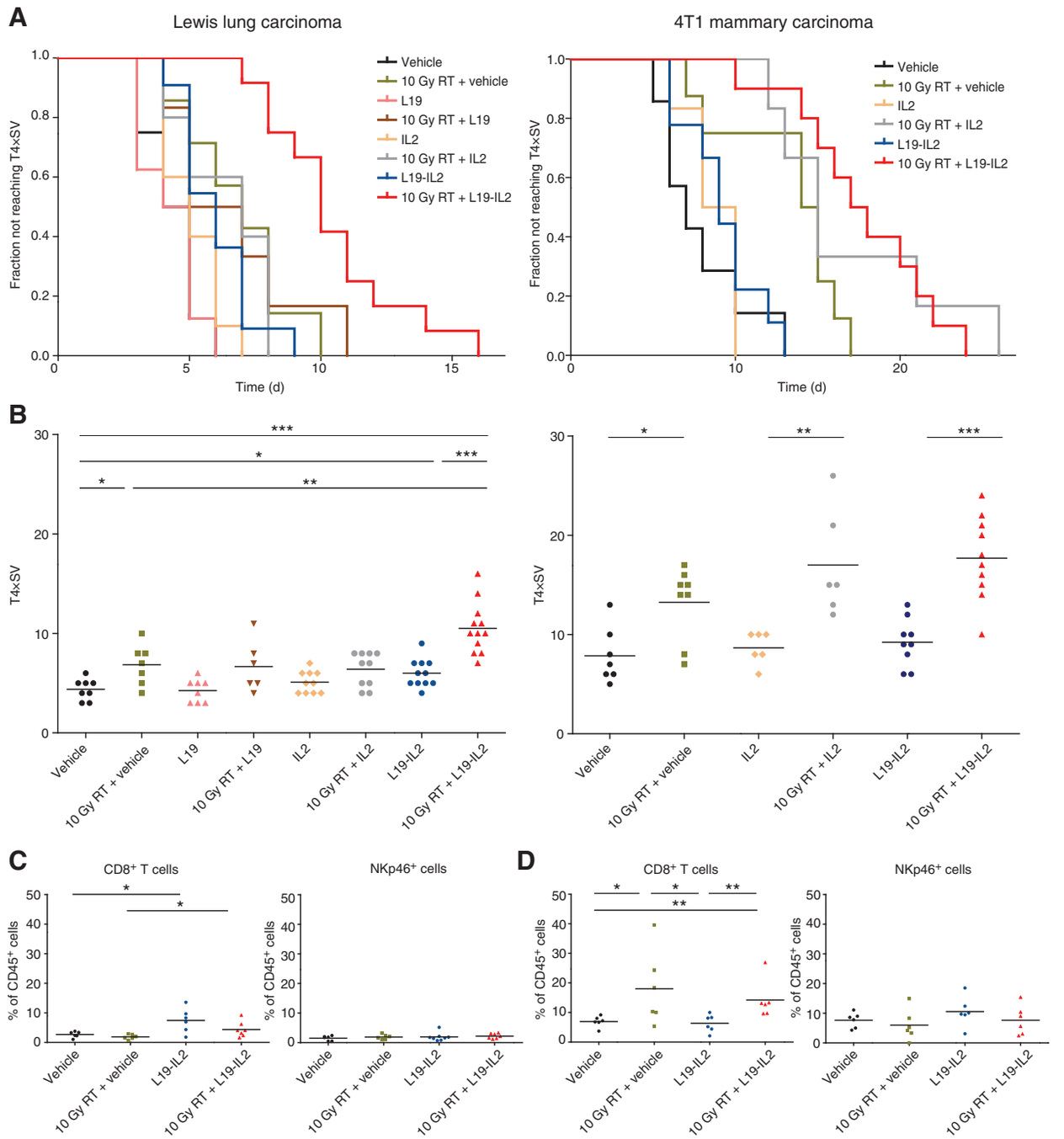

Figure 3.
Combination therapy results in an additive effect in the LLC model (intermediate ED-B) and no effect in the 4T1 model (low ED-B). A, survival curves of the LLC and 4T1 models, showing the fraction of tumors not reaching 4 times start volume (T4 × SV). B, scatter plots of the LLC and 4T1 models, showing the time to reach 4 times start volume (T4 × SV). Flow cytometric analyses of tumor leukocyte content in the LLC (C) and 4T1 (D) models, showing the percentage of $CD8^+$ and $NKp46^+$ cells of all $CD45^+$ cells in the tumor. *, $P < 0.05$; **, $P < 0.01$; ***, $P < 0.001$.

Combination therapy results in complete remission of 75% in the C51 model

We evaluated the time to reach four times start volume (T4 × SV) for all treatment groups in the C51 model with high ED-B expression. Experiments were started at an average tumor volume of 254 ± 126 mm^3. L19, IL2, or L19-IL2 monotherapy increased the T4 × SV to 6.1 ± 0.9 ($P < 0.01$), 6.3 ± 1.2 ($P < 0.01$), and 6.0 ± 1.6 days ($P < 0.05$), respectively, as compared with the vehicle (4.8 ± 0.8 days) treated C51 tumor-bearing animals, but no significant differences between these three

Published OnlineFirst December 31, 2014; DOI: 10.1158/1078-0432.CCR-14-2676

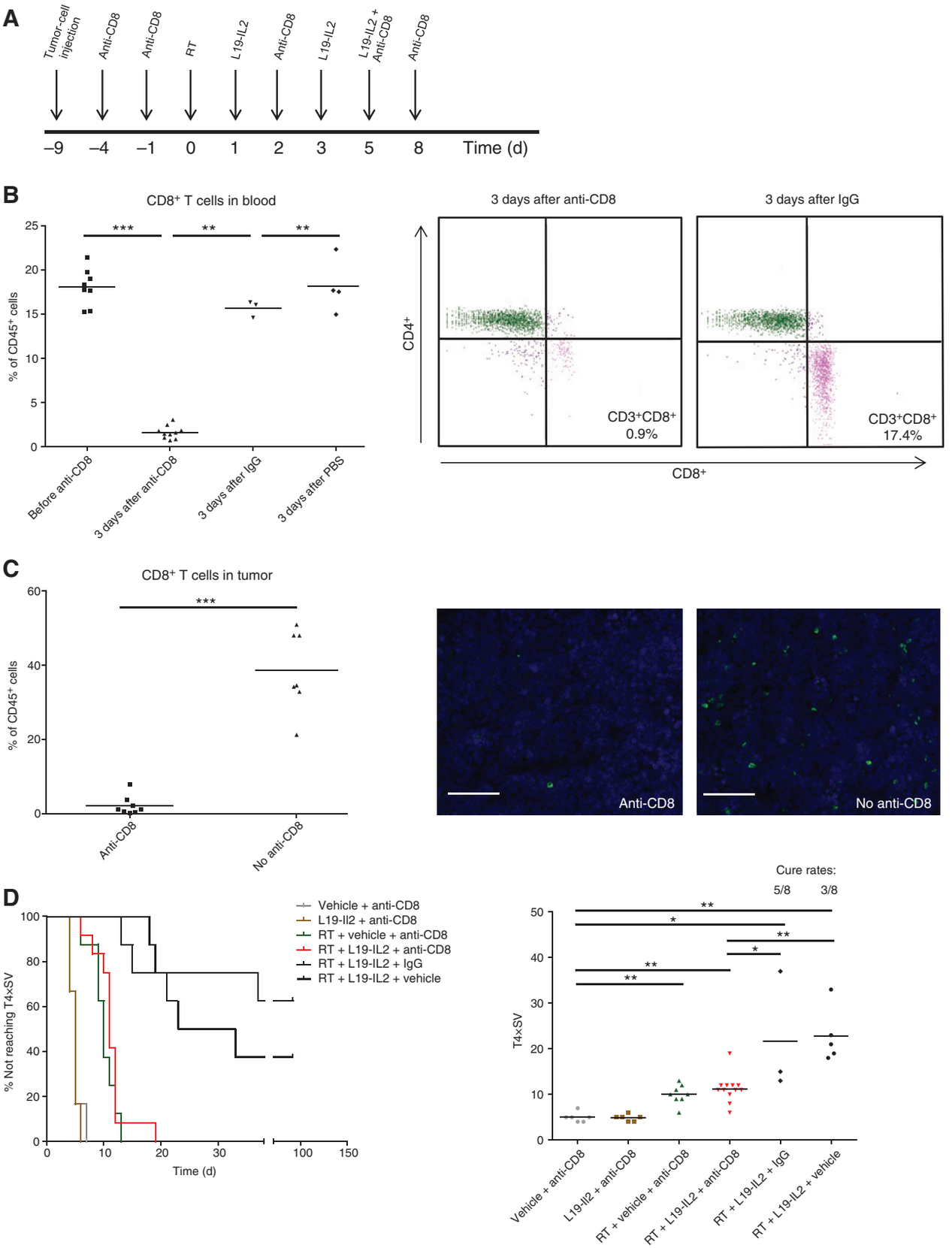

Published OnlineFirst December 31, 2014; DOI: 10.1158/1078-0432.CCR-14-2676

treatment groups were observed. Single-dose radiotherapy (10 Gy) significantly enhanced tumor growth delay when preceding vehicle ($P < 0.001$), L19 ($P < 0.001$), or IL2 ($P < 0.001$) treatment. Upon combination with L19-IL2 therapy, a highly significant ($P < 0.0001$) synergistic antitumor effect was observed with 9/12 cures (Fig. 2A and B). Reduction of the single-dose radiations to 5 or 2 Gy showed a dose-dependent treatment effect. For tumors treated with the combination of ionizing radiation and L19-IL2, a cure rate of 6/12 and 1/12 was observed for irradiation with 5 Gy ($P < 0.001$) and 2 Gy ($P = 0.002$), respectively, as compared with the combination with vehicle treatment (Fig. 2A and B).

FACS analysis was performed to evaluate the underlying immunologic parameters. The percentage of baseline cytotoxic T cells in the tumor was 22.2% ± 9.2% of $CD45^+$ cells in vehicle-treated animals. Radiotherapy slightly enhanced the cytotoxic T-cell subpopulation (28.1% ± 5.7%), without being significant ($P = 0.24$). The percentage of cytotoxic T cells during combination treatment was significantly higher than in vehicle (38.6% ± 10.8%, $P < 0.01$) or L19-IL2 only (22.0% ± 8.8%, $P = 0.01$) treated animals. There was no significant difference in the $CD45^+$ population in the tumor between different treatment groups. In addition, no significant differences were observed in $NKp46^+$ NK cells, $CD4^+$ T cells, or $CD19^+$ B cells between the treatment groups (Fig. 2C; Supplementary Table S1). Flow cytometry of the lymph node and spleen tissue showed no significant difference for any of the analyzed immune subpopulations ($CD8^+$, $CD4^+$, $CD19^+$, and NK; Supplementary Table S1).

Combination therapy results in increased growth delay in the LLC model

Next, we investigated the possible therapeutic effect of combined radiotherapy with L19-IL2 in the LLC model with intermediate ED-B expression. Experiments were started at an average tumor volume of 254 ± 148 mm^3. There was no significant difference in tumor growth delay for L19 (4.3 ± 1.2 days) or IL2 (5.1 ± 1.1 days) compared with vehicle (4.4 ± 1.1 days) treated animals. L19-IL2 monotherapy resulted in a significant tumor growth delay ($P = 0.02$), increasing T4 × SV to 6.0 ± 1.4 days. Single-dose radiotherapy (10 Gy) only also showed an increased growth delay (6.9 ± 2.0 days; $P = 0.02$), however, the combination of radiotherapy with L19-IL2 resulted in the largest growth delay (10.5 ± 2.6). This was significantly longer than after radiotherapy or L19-IL2 only ($P < 0.01$ and $P < 0.001$, respectively; Fig. 3A and B). There was no significant interaction between radiotherapy and L19-IL2 (two-way ANOVA; $P = 0.15$), the effect of the combination therapy in LLC was additive.

The observed baseline percentage of cytotoxic $CD8^+$ T cells in this LLC model was significantly lower than in the C51 model ($P = 0.002$). The number of cytotoxic T cells as a percentage of $CD45^+$ cells increased significantly upon L19-IL2 treatment: from 2.7% ± 1.0% (vehicle) to 7.4% ± 4.1% (L19-IL2, $P = 0.04$), and from 1.9% ± 0.8% (radiotherapy) to 4.4% ± 2.6% (radiotherapy+L19-IL2, $P = 0.04$; Fig. 3C). Radiation caused a significant decrease in the percentage of $CD19^+$ and $CD4^+$ cells in the tumor compared with vehicle treatment (Supplementary Table S1). No differences were observed in the percentage of $NKp46^+$ cells in the tumor (Fig. 3C). Analysis of the lymph nodes and spleen tissue showed no significant differences (Supplementary Table S1).

In the low/negative ED-B–expressing 4T1 model, the addition of L19-IL2 to radiotherapy has no effect

Next, we investigated whether L19-IL2 had any off-target effects using the low ED-B–expressing 4T1 model. Experiments were started at an average tumor volume of 152 ± 48 mm^3. For the 4T1 model, no statistically significant differences were observed between vehicle, IL2 and L19-IL2–treated animals, with an average T4 × SV of 7.9 ± 2.8, 8.7 ± 1.6, and 9.2 ± 2.4 days, respectively. Single-dose radiotherapy (10 Gy) increased growth delay significantly for all treatment groups: radiotherapy + vehicle (13.3 ± 3.7 days, $P = 0.01$), radiotherapy + IL2 (17.0 ± 5.4 days, $P < 0.01$), or radiotherapy + L19-IL2 (17.7 ± 4.2 days, $P < 0.001$); however, no statistically significant differences ($P = 0.47$ and $P = 0.59$) were observed between these irradiated groups (Fig. 3A and B). There is no significant interaction between radiotherapy and L19-IL2 (two-way ANOVA; $P = 0.20$).

Radiotherapy caused a significant increase in the presence of $CD8^+$ T cells in the 4T1 tumor. The percentage of $CD8^+$ T cells increased from 6.9 ± 1.8 (vehicle) to 18.0 ± 12.6 (radiotherapy + vehicle, $P = 0.04$) and from 6.4 ± 2.9 (L19-IL2) to 14.2 ± 6.4 (radiotherapy + L19-IL2, $P < 0.01$). Albeit, no significant differences ($P = 1.0$) were observed for L19-IL2–treated animals compared with vehicle. No significant differences were observed for the percentage of NK cells in the tumor for any of the treatment groups (Fig. 3D). The percentage of $CD19^+$ cells were significantly higher for treatment with L19-IL2 alone (4.0 ± 1.6) compared with vehicle (2.5 ± 0.6, $P = 0.03$), radiotherapy + vehicle (2.0 ± 0.7, $P = 0.02$), and radiotherapy + L19-IL2 (1.6 ± 1.2, $P = 0.04$; Supplementary Table S1). Analysis of the spleen and lymph nodes showed no significant difference for any of the analyzed immune cells.

Depletion of cytotoxic T cells prohibits complete remission

On the basis of our observation that radiotherapy + L19-IL2 immunotherapy significantly increases the $CD8^+$ T-cell subpopulation, we assessed the causal relationship between the therapeutic effect and $CD8^+$ T cells by depleting the $CD8^+$ T cells in the C51 tumor model. Tumor cell injection did not result in changed immune subpopulations. Treatment with the $CD8^+$ T-cell depleting (JTS169) antibody abolished $CD8^+$ T cells in the blood 2 days after injection (0.06% ± 0.06%; >99% depletion). Cytotoxic $CD8^+$ T cells were detectable again at day 3 (1.6% ± 0.7%) after

Figure 4.
Depletion of cytotoxic T cells prohibits complete remission in the C51 model. A, cartoon of treatment schedule. B, % $CD8^+$ cells of $CD45^+$ cells 3 days after intraperitoneal anti-CD8, IgG, or PBS (vehicle) and an example of the flow cytometry results showing the percentage of $CD3^+CD8^+$ cells present in the blood 3 days after anti-CD8 or IgG administration. C, % of $CD8^+$ cells present in the tumor of CD8-depleted and nondepleted mice treated with radiotherapy and L19-IL2 analyzed by flow cytometry and an immunofluorescent CD8 staining (green), cell nuclei stained with DAPI (blue). D, fraction of tumors not reacting 4 times start volume (T4 × SV) and time to reach T4 × SV for the different treatment groups. *, $P < 0.05$; **, $P < 0.01$; ***, $P < 0.001$.

Published OnlineFirst December 31, 2014; DOI: 10.1158/1078-0432.CCR-14-2676

depletion and levels increased over time to 5.7% ± 3.0% at day 5 (Supplementary Fig. S4A). On the basis of these data, we opted for 3 daily administrations of $CD8^+$ depleting antibody to effect sustained ablation of $CD8^+$ T cells (Fig. 4A). Three days after depletion with 0.2 mg anti-CD8 antibody, the $CD8^+$ T-cell population was significantly reduced in blood ($P < 0.0001$), whereas the control groups receiving either isotype IgG (15.7% ± 0.9%) or vehicle (18.1% ± 3.1%) showed similar numbers of $CD8^+$ cells as baseline (Fig. 4B). $CD8^+$ T cells were also depleted in the tumor (2.2% ± 2.6%, vs. 38.6% ± 10.8% at baseline; Fig. 4C), spleen, and lymph nodes (Supplementary Fig. S4B). Upon depletion of cytotoxic T cells, the combination of radiotherapy with L19-IL2 lost its therapeutic effect (T4 × SV = 11.25 ± 3.0 days) and was not superior ($P = 0.31$) to radiotherapy only (T4 × SV = 10.0 ± 3.0 days). However, in agreement with previous results, the animals in the control groups (without $CD8^+$ T-cell depletion), still showed sustained antitumor effects (IgG: cure 5/8, vehicle: cure 3/8) after 10 Gy irradiation and L19-IL2 (Fig. 4D).

Discussion

Radiation-induced cell death is an immunogenic process that can be used to initiate tumor-specific immune responses (39). The selective delivery of IL2 to tumor vascular components is promising in cancer immunotherapy (16, 40, 41) and may be used to enhance the therapeutic potential of radiotherapy. We hypothesized that the combination of radiotherapy with the targeted immunocytokine L19-IL2 may cause an enhanced antitumor effect dependent on the expression of ED-B. In this study, we assessed the therapeutic potential and underlying mechanisms of the combination therapy in three different tumor models with varying ED-B expression.

On the basis of growth delay experiments, the combination therapy showed a therapeutic gain compared with the single treatment arms, with an additive effect for the LLC model and a long-lasting highly synergistic effect for the C51 model for which a cure rate of 75% was observed. As expected, no effect was observed for the 4T1 model, which has a low ED-B expression. The results show that ED-B expression is essential for the efficacy of combined irradiation and L19-IL2 administration. The C51 model showed the highest ED-B expression and the most promising results for the combination therapy suggesting that high ED-B expression may assure better L19-IL2 tumor targeting. Like our C51 model, ED-B is overexpressed in many solid tumors (25–27, 29, 41), which makes this combination therapy (radiotherapy + L19-IL2) potentially interesting for the majority of cancer types.

The highly synergistic effect observed in the C51 model upon radiotherapy and tumor-targeted L19-IL2 treatment is in agreement with previous results described by Yasuda and colleagues (23). They observed a complete eradication of a colon carcinoma cell line (Colon26) in Balb/c mice after the combination of radiotherapy with intratumoral injections with IL2. For the models presented in this study, no additional benefit was observed for the use of the single treatment with L19-IL2 in comparison with IL2 treatment. This is in contradiction with the results from previous studies, showing that L19-IL2 provides a stronger antitumor effect compared with equimolar dosing of untargeted IL2 in an F9 teratocarcinoma or a human pancreatic carcinoma xenograft model (16, 42). This might be explained by the use of different mouse strains, tumor models, and treatment schedules. However, in combination with radiotherapy, we did find a stronger antitumor effect when using L19-IL2 compared with IL2. This shows that, in agreement with previous results, L19-IL2 has an increased antitumor effect.

Upon combination therapy, an increased number of cytotoxic T cells was observed in the tumor of the LLC and C51 models. A comparison between the used models shows that already at baseline, the number of cytotoxic T cells is higher for the C51 model than for the LLC and 4T1 models. Results are in agreement with previous publications, where it was already shown that, dependent on tumor model, the efficacy of IL2 treatment can be based on T cells (43, 44), or a combination of NK and T cells (16). In mice bearing C51 colon carcinoma, L19-IL2 as single treatment already showed an increased number of tumor-infiltrating cytotoxic T cells and NK cells in immunohistochemical analysis (16). This was confirmed in the clinical setting where both cell types were upregulated in the peripheral blood of patients as a result of L19-IL2 treatment (34). Johnson and colleagues (45) combined an alternative immunocytokine, KS-IL2, with radiofrequency ablation in a murine colon adenocarcinoma (CT26). The combination increased growth suppression, and a greater proportion of $CD4^+$ and $CD8^+$ cells was observed. Furthermore, the therapeutic effect of IL2 coupled to the human monocloncal antibodies F8 and F16 that recognize the ED-A and ED-B domains of fibronectin and the A1 domain of tenascin-C, respectively, was shown to be mediated by $CD8^+$ and NK cells in an *in vivo* AML model (46). Moreover, the antibody-based targeted delivery of IL4 and IL12 to tumor neovasculature has also been shown to eradicate tumors by both NK and $CD8^+$ T cells (47). In our study, we irradiated the tumors before administration of the immunocytokine L19-IL2. It is known that radiotherapy can promote a DC-mediated cytotoxic T-lymphocyte (CTL) response, the so-called immunogenic cell death (48). This form of cell death may be further enhanced by the targeted delivery of IL2 to the irradiated tumors. Our combination therapy may therefore favor the CTL response, because NK cells are able to detect and destroy malignant and virally infected cells directly (15). Indeed, we have shown that depletion of the cytotoxic T cells in the C51 model inhibits the antitumor effect after combination therapy, providing evidence that the complete remission observed in the majority of C51 tumors, is attributed to the high number of cytotoxic T cells present in the tumor after combination therapy.

Evidence suggests that local radiation always elicits activation of the immune system, even though the proportion of tumor cells undergoing immunogenic cell death will vary (5, 7). Demaria and colleagues (7) showed that a single low dose of radiotherapy (2 Gy) in combination with Flt3-Ligand (enhancing the number of available dendritic cells) could already trigger antitumor T-cell responses, while Schaue and colleagues (49) reported that only doses above 7.5 Gy were immunostimulatory. To test this in our study, the radiotherapy dose was reduced from 10 Gy to 5 Gy or 2 Gy for the C51 model. The decrease in dose of irradiation resulted in a reduced number of tumor eradications, showing that in this model and experimental set-up the radiotherapy dose is an important parameter to generate cure. We therefore suggest that a minimal radiotherapy dose is necessary to provide sufficient immunogenic cell death to trigger the antitumor immune response. In our experiments, we only tested one single radiotherapy dose in combination with

L19-IL2, showing excellent results. Therefore, we expect that the use of a few high doses of radiotherapy (SBRT) is sufficient to release DAMPs and initiate the antitumor immune response, while limiting the damage to essential immunologic ($CD8^+$) cells. In a previous clinical trial, Seung and colleagues (50) combined SBRT with systemic IL2 in patients with metastatic melanoma or RCC, which already provided a higher response rate compared to historical data. On the basis of our results, the use of L19-IL2, instead of systemic IL2, will increase the potential and decrease toxicity. Therefore, the clinical set-up combining SBRT with L19-IL2 seems very promising and will be investigated in a clinical trial (NCT02086721).

As ED-B has an identical amino sequence in mice and humans, the human single-chain Fv monoclonal antibody fragment L19 combined with IL2 can be directly used in clinical setting. In phase I trials, L19-IL2 was already safely administered in melanoma and renal cell carcinoma, even in combination with decarbazine, which is not an ICD inducer like radiotherapy (34–36). On the basis of our current results that ED-B expression is essential to obtain a therapeutic benefit, L19-SIP imaging should be included in a clinical trial set-up to evaluate the possibility to select patients for L19-IL2 treatment. However, the ultimate aim is to increase progression-free survival by the irradiation of accessible, larger solid tumors/metastasis, initiating an antitumor immune response that will attack the solid lesions and its micrometastasis.

In conclusion, the combination therapy of radiotherapy with L19-IL2 can enhance the immune response against diverse solid tumors, providing an additive or synergistic antitumor effect in the presence of ED-B. These findings can directly be translated to a phase I clinical study in patients with an oligometastatic solid tumor, because the use of L19-IL2 is proven to be safe in patients. This promising new opportunity for cancer treatment is subject of clinical investigation.

Disclosure of Potential Conflicts of Interest

D. Neri is an employee of, has ownership interest (including patents) in, and is a consultant/advisory board member for Philogen. No potential conflicts of interest were disclosed by the other authors.

Authors' Contributions

Conception and design: C.M.L. Zegers, N.H. Rekers, W.T.V. Germeraad, D. Neri, E.G.C. Troost, L.J. Dubois, P. Lambin

Development of methodology: C.M.L. Zegers, N.H. Rekers, L.J. Dubois, P. Lambin

Acquisition of data (provided animals, acquired and managed patients, provided facilities, etc.): C.M.L. Zegers, N.H. Rekers, D.H.F. Quaden, N.G. Lieuwes, A. Yaromina, L. Wieten, E.A.L. Biessen, L. Boon, L.J. Dubois

Analysis and interpretation of data (e.g., statistical analysis, biostatistics, computational analysis): C.M.L. Zegers, N.H. Rekers, D.H.F. Quaden, A. Yaromina, W.T.V. Germeraad, L. Wieten, E.G.C. Troost, L.J. Dubois, P. Lambin

Writing, review, and/or revision of the manuscript: C.M.L. Zegers, N.H. Rekers, A. Yaromina, W.T.V. Germeraad, L. Wieten, E.A.L. Biessen, L. Boon, D. Neri, E.G.C. Troost, L.J. Dubois, P. Lambin

Administrative, technical, or material support (i.e., reporting or organizing data, constructing databases): C.M.L. Zegers, N.H. Rekers, N.G. Lieuwes

Study supervision: L.J. Dubois, P. Lambin

Acknowledgments

The authors thank S.D. Heijnen for the professional revision of the article.

Grant Support

This study was financially supported by Philogen S.p.A., EU 6th and 7th framework program (METOXIA, ARTFORCE), and The Netherlands Organisation for Scientific Research (NWO), grant number 911-06-003.

The costs of publication of this article were defrayed in part by the payment of page charges. This article must therefore be hereby marked *advertisement* in accordance with 18 U.S.C. Section 1734 solely to indicate this fact.

Received October 22, 2014; revised December 11, 2014; accepted December 11, 2014; published OnlineFirst December 31, 2014.

References

1. Krysko DV, Garg AD, Kaczmarek A, Krysko O, Agostinis P, Vandenabeele P. Immunogenic cell death and DAMPs in cancer therapy. Nat Rev Cancer 2012;12:860–75.
2. Kaur P, Asea A. Radiation-induced effects and the immune system in cancer. Front Oncol 2012;2:191.
3. Demaria S, Bhardwaj N, McBride WH, Formenti SC. Combining radiotherapy and immunotherapy: a revived partnership. Int J Radiat Oncol Biol Phys 2005;63:655–66.
4. McBride WH, Chiang CS, Olson JL, Wang CC, Hong JH, Pajonk F, et al. A sense of danger from radiation. Radiat Res 2004;162:1–19.
5. Demaria S, Formenti SC. Role of T lymphocytes in tumor response to radiotherapy. Front Oncol 2012;2:95.
6. Green DR, Ferguson T, Zitvogel L, Kroemer G. Immunogenic and tolerogenic cell death. Nat Rev Immunol 2009;9:353–63.
7. Demaria S, Ng B, Devitt ML, Babb JS, Kawashima N, Liebes L, et al. Ionizing radiation inhibition of distant untreated tumors (abscopal effect) is immune mediated. Int J Radiat Oncol Biol Phys 2004;58:862–70.
8. Wersall PJ, Blomgren H, Pisa P, Lax I, Kalkner KM, Svedman C. Regression of non-irradiated metastases after extracranial stereotactic radiotherapy in metastatic renal cell carcinoma. Acta Oncol 2006;45:493–7.
9. Okuma K, Yamashita H, Niibe Y, Hayakawa K, Nakagawa K. Abscopal effect of radiation on lung metastases of hepatocellular carcinoma: a case report. J Med Case Rep 2011;5:111.
10. Cotter SE, Dunn GP, Collins KM, Sahni D, Zukotynski KA, Hansen JL, et al. Abscopal effect in a patient with metastatic Merkel cell carcinoma following radiation therapy: potential role of induced antitumor immunity. Arch Dermatol 2011;147:870–2.
11. Kachikwu EL, Iwamoto KS, Liao YP, DeMarco JJ, Agazaryan N, Economou JS, et al. Radiation enhances regulatory T cell representation. Int J Radiat Oncol Biol Phys 2011;81:1128–35.
12. Postow MA, Harding J, Wolchok JD. Targeting immune checkpoints: releasing the restraints on anti-tumor immunity for patients with melanoma. Cancer J 2012;18:153–9.
13. Stamell EF, Wolchok JD, Gnjatic S, Lee NY, Brownell I. The abscopal effect associated with a systemic anti-melanoma immune response. Int J Radiat Oncol Biol Phys 2013;85:293–5.
14. Topham NJ, Hewitt EW. Natural killer cell cytotoxicity: how do they pull the trigger? Immunology 2009;128:7–15.
15. Janeway CA, Travers P, Walport M, Shlomchik MJ. Immunobiology: The Immune System in Health and Disease. 5th edition ed: Garland Science, New York, NY; 2001.
16. Carnemolla B, Borsi L, Balza E, Castellani P, Meazza R, Berndt A, et al. Enhancement of the antitumor properties of interleukin-2 by its targeted delivery to the tumor blood vessel extracellular matrix. Blood 2002;99:1659–65.
17. Wang KS, Ritz J, Frank DA. IL-2 induces STAT4 activation in primary NK cells and NK cell lines, but not in T cells. J Immunol 1999;162:299–304.
18. Krause M, Schmitz M, Noessner E, Skrablin PS, Wehner R, Rieber EP, et al. Adoptive transfer of cytotoxic T-cells for treatment of residual disease after irradiation. Int J Radiat Biol 2007;83:827–36.
19. Payne R, Glenn L, Hoen H, Richards B, Smith JW II, Lufkin R, et al. Durable responses and reversible toxicity of high-dose interleukin-2 treatment of melanoma and renal cancer in a Community Hospital Biotherapy Program. J Immunother Cancer 2014;2:13.

Published OnlineFirst December 31, 2014; DOI: 10.1158/1078-0432.CCR-14-2676

20. Alwan LM, Grossmann K, Sageser D, Van Atta J, Agarwal N, Gilreath JA. Comparison of acute toxicity and mortality after two different dosing regimens of high-dose interleukin-2 for patients with metastatic melanoma. Target Oncol 2014;9:63–71.
21. Den Otter W, Jacobs JJ, Battermann JJ, Hordijk GJ, Krastev Z, Moiseeva EV, et al. Local therapy of cancer with free IL-2. Cancer Immunol Immunother 2008;57:931–50.
22. Jacobs JJ, Sparendam D, Den Otter W. Local interleukin 2 therapy is most effective against cancer when injected intratumourally. Cancer Immunol Immunother 2005;54:647–54.
23. Yasuda K, Nirei T, Tsuno NH, Nagawa H, Kitayama J. Intratumoral injection of interleukin-2 augments the local and abscopal effects of radiotherapy in murine rectal cancer. Cancer Sci 2011;102:1257–63.
24. Kontermann RE. Antibody-cytokine fusion proteins. Arch Biochem Biophys 2012;526:194–205.
25. Kaczmarek J, Castellani P, Nicolo G, Spina B, Allemanni G, Zardi L. Distribution of oncofetal fibronectin isoforms in normal, hyperplastic and neoplastic human breast tissues. Int J Cancer 1994;59:11–6.
26. D'Ovidio MC, Mastracchio A, Marzullo A, Ciabatta M, Pini B, Uccini S, et al. Intratumoral microvessel density and expression of ED-A/ED-B sequences of fibronectin in breast carcinoma. Eur J Cancer 1998;34:1081–5.
27. Pujuguet P, Hammann A, Moutet M, Samuel JL, Martin F, Martin M. Expression of fibronectin ED-A+ and ED-B+ isoforms by human and experimental colorectal cancer. Contribution of cancer cells and tumor-associated myofibroblasts. Am J Pathol 1996;148:579–92.
28. Santimaria M, Moscatelli G, Viale GL, Giovannoni L, Neri G, Viti F, et al. Immunoscintigraphic detection of the ED-B domain of fibronectin, a marker of angiogenesis, in patients with cancer. Clin Cancer Res 2003;9:571–9.
29. El-Emir E, Dearling JL, Huhalov A, Robson MP, Boxer G, Neri D, et al. Characterisation and radioimmunotherapy of L19-SIP, an anti-angiogenic antibody against the extra domain B of fibronectin, in colorectal tumour models. Br J Cancer 2007;96:1862–70.
30. Galler K, Junker K, Franz M, Hentschel J, Richter P, Gajda M, et al. Differential vascular expression and regulation of oncofetal tenascin-C and fibronectin variants in renal cell carcinoma (RCC): implications for an individualized angiogenesis-related targeted drug delivery. Histochem Cell Biol 2012;137:195–204.
31. Rossin R, Berndorff D, Friebe M, Dinkelborg LM, Welch MJ. Small-animal PET of tumor angiogenesis using a (76)Br-labeled human recombinant antibody fragment to the ED-B domain of fibronectin. J Nucl Med 2007;48:1172–9.
32. Tijink BM, Perk LR, Budde M, Stigter-van Walsum M, Visser GW, Kloet RW, et al. (124)I-L19-SIP for immuno-PET imaging of tumour vasculature and guidance of (131)I-L19-SIP radioimmunotherapy. Eur J Nucl Med Mol Imaging 2009;36:1235–44.
33. Balza E, Carnemolla B, Mortara L, Castellani P, Soncini D, Accolla RS, et al. Therapy-induced antitumor vaccination in neuroblastomas by the combined targeting of IL-2 and TNFalpha. Int J Cancer 2010;127:101–10.
34. Johannsen M, Spitaleri G, Curigliano G, Roigas J, Weikert S, Kempkensteffen C, et al. The tumour-targeting human L19-IL2 immunocytokine: preclinical safety studies, phase I clinical trial in patients with solid tumours and expansion into patients with advanced renal cell carcinoma. Eur J Cancer 2010;46:2926–35.
35. Eigentler TK, Weide B, de Braud F, Spitaleri G, Romanini A, Pflugfelder A, et al. A dose-escalation and signal-generating study of the immunocytokine L19-IL2 in combination with dacarbazine for the therapy of patients with metastatic melanoma. Clin Cancer Res 2011;17:7732–42.
36. Hervieu A, Mignot G, Ghiringhelli F. Dacarbazine mediate antimelanoma effects via NK cells. Oncoimmunology 2013;2:e23714.
37. Pfaffen S, Frey K, Stutz I, Roesli C, Neri D. Tumour-targeting properties of antibodies specific to MMP-1A, MMP-2 and MMP-3. Eur J Nucl Med Mol Imaging 2010;37:1559–65.
38. Edelstein A, Amodaj N, Hoover K, Vale R, Stuurman N. Computer control of microscopes using microManager. Curr Protoc Mol Biol 2010;Chapter 14:Unit14 20.
39. Kamrava M, Bernstein MB, Camphausen K, Hodge JW. Combining radiation, immunotherapy, and antiangiogenesis agents in the management of cancer: the Three Musketeers or just another quixotic combination? Mol Biosyst 2009;5:1262–70.
40. Schliemann C, Palumbo A, Zuberbuhler K, Villa A, Kaspar M, Trachsel E, et al. Complete eradication of human B-cell lymphoma xenografts using rituximab in combination with the immunocytokine L19-IL2. Blood 2009;113:2275–83.
41. Menrad A, Menssen HD. ED-B fibronectin as a target for antibody-based cancer treatments. Expert Opin Ther Targets 2005;9:491–500.
42. Wagner K, Schulz P, Scholz A, Wiedenmann B, Menrad A. The targeted immunocytokine L19-IL2 efficiently inhibits the growth of orthotopic pancreatic cancer. Clin Cancer Res 2008;14:4951–60.
43. Becker JC, Pancook JD, Gillies SD, Furukawa K, Reisfeld RA. T cell-mediated eradication of murine metastatic melanoma induced by targeted interleukin 2 therapy. J Exp Med 1996;183:2361–6.
44. Xiang R, Lode HN, Dolman CS, Dreier T, Varki NM, Qian X, et al. Elimination of established murine colon carcinoma metastases by antibody-interleukin 2 fusion protein therapy. Cancer Res 1997;57:4948–55.
45. Johnson EE, Yamane BH, Buhtoiarov IN, Lum HD, Rakhmilevich AL, Mahvi DM, et al. Radiofrequency ablation combined with KS-IL2 immunocytokine (EMD 273066) results in an enhanced antitumor effect against murine colon adenocarcinoma. Clin Cancer Res 2009;15:4875–84.
46. Gutbrodt KL, Schliemann C, Giovannoni L, Frey K, Pabst T, Klapper W, et al. Antibody-based delivery of interleukin-2 to neovasculature has potent activity against acute myeloid leukemia. Sci Transl Med 2013;5:201ra118.
47. Hemmerle T, Neri D. The antibody-based targeted delivery of interleukin-4 and 12 to the tumor neovasculature eradicates tumors in three mouse models of cancer. Int J Cancer 2014;134:467–77.
48. Apetoh L, Ghiringhelli F, Tesniere A, Obeid M, Ortiz C, Criollo A, et al. Toll-like receptor 4-dependent contribution of the immune system to anticancer chemotherapy and radiotherapy. Nat Med 2007;13:1050–9.
49. Schaue D, Ratikan JA, Iwamoto KS, McBride WH. Maximizing tumor immunity with fractionated radiation. Int J Radiat Oncol Biol Phys 2012;83:1306–10.
50. Seung SK, Curti BD, Crittenden M, Walker E, Coffey T, Siebert JC, et al. Phase 1 study of stereotactic body radiotherapy and interleukin-2–tumor and immunological responses. Sci Transl Med 2012;4:137ra74.

AACR American Association for Cancer Research

Clinical Cancer Research

Radiotherapy Combined with the Immunocytokine L19-IL2 Provides Long-lasting Antitumor Effects

Catharina M.L. Zegers, Nicolle H. Rekers, Dana H.F. Quaden, et al.

Clin Cancer Res 2015;21:1151-1160. Published OnlineFirst December 31, 2014.